Research Article | Vol. 12, No. 5 / 1 May 2021 / Biomedical Optics Express 2902
Biomedical Optics EXPRESS

Visual performance after the deterioration of retinal image quality: induced forward scattering using Bangerter foils and fog filters

JOSÉ J. CASTRO-TORRES,* FRANCESCO MARTINO, MIRIAM CASARES-LÓPEZ, SONIA ORTIZ-PEREGRINA, AND CAROLINA ORTIZ

Laboratory of Vision Sciences and Applications, Department of Optics, University of Granada, 18071 Granada, Spain
jjcastro@ugr.es

Abstract: We induced and evaluated different levels of retinal-image degradation using Bangerter foils and fog filters. We found increased straylight and an important deterioration in visual performance, assessed by means of visual acuity, contrast threshold, and visual discrimination capacity. Bangerter foils induced forward scattering levels comparable to those observed in mature to severe cataracts, with an important impact of halos and starbursts. Fog filters induced lower levels of intraocular scattering, although luminous veils and circular halos were reported. The visual disturbance index positively correlated with intraocular scattering and straylight. Our results show retinal-image quality has an important influence on night-vision performance.

1. Introduction

In recent years, research into retinal-image quality has increased, mainly due to its clinical applications, especially in terms of refractive and cataract surgery [1–4] and ocular pathologies [5–8]. The characterization of the eye in older adults is another important clinical application, considering the age-related deterioration of the ocular media [9,10]. It is well known that the optical conditions of the ocular media have an important effect on the retinal-image quality of the human eye. In fact, light scattering through the ocular media is the most important cause of retinal-image degradation, especially in eye diseases such as cataracts [8,11]. In the presence of a light source, light is scattered when passing through the ocular media, leading to increased straylight. This amplification of scattered light may produce certain visual disturbances caused by the straylight, especially under low-illumination conditions, such as disability glare [12], thus reducing night-vision performance. In disability glare, the visual field luminance is greater than that for which the eyes are adapted, causing annoyance and discomfort [13]. Moreover, intraocular straylight induced by light scattering reduces the overall contrast of the retinal image and, consequently, some visual functions, such as contrast sensitivity [14,15] and visual discrimination capacity (halo perception) [11,16], are deteriorated. These negative effects are more evident when the source of glare is present within the visual field [17]. Some studies have found a greater deterioration in eyes with a poorer retinal-image quality [5,6,10,18]. Most previous work is focused on the study of visual acuity and contrast sensitivity. There has been scant analysis of other important visual functions, such as glare sensitivity, halo perception, and visual discrimination capacity. However, as we have mentioned, intraocular scattering and straylight produce important visual disturbances, especially under conditions of glare or in dim surroundings, which could have repercussions on daily tasks like driving [16]. For this reason, quantifying positive dysphotopsias such as glare, halos, and starbursts, is particularly interesting for both research and clinical purposes [12,14,19,20].

#424715 https://doi.org/10.1364/BOE.424715
Journal © 2021 Received 10 Mar 2021; revised 15 Apr 2021; accepted 19 Apr 2021; published 23 Apr 2021

Biomedical Optics EXPRESS

On the other hand, from a clinical perspective, it is interesting to analyze, in the same patient, how different levels of retinal-image degradation influence visual performance, as well as the correlation between retinal-image quality and visual function. In this sense, simulating the degradation of retinal quality is a useful tool for research purposes with potential clinical applications, particularly for evaluating visual function and ocular parameters, and studying and monitoring several ocular pathologies [21–24]. In order to quantify and evaluate visual performance, including the characterization of dysphotopsias (glare, halos, etc.), filters like Bangerter foils, and certain camera fog filters, can be used to simulate different levels of retinal image quality degradation. Bangerter foils are widely used as occlusions for penalization in children undergoing amblyopia therapy [25,26]. Some authors have used Bangerter foils to optically characterize the eye or simulate optical degradation [24,27,28]. In addition, some camera fog filters have been proved to simulate incipient and moderate cataracts, due to the induced forward scattering [23,29,30].

In this study, we induced and evaluated different levels of retinal-image degradation by increasing forward scattering, using several Bangerter foils and fog filters. In addition, we studied the influence of this retinal-image degradation on visual performance by means of visual acuity, contrast threshold (under normal and glare conditions), straylight, and visual discrimination capacity (perception of halos). To this end, we also analyzed possible correlations between night-vision performance and retinal-image quality.

2. Methods

2.1. Subjects

A total of 7 subjects (fourteen eyes) were enrolled in the experiment (3 females, 4 males) with a mean age of 27.7 ± 6.5 years. The admission criteria for the subjects were: decimal visual acuity ≥ 1.0 with the best correction for both eyes, and no pathological conditions or pharmacological treatments that could affect visual performance. All participants gave their informed consent in accordance with the Helsinki Declaration, and the study was approved by the Human Research Ethics Committee of the University of Granada (921/CEIH/2019). Corrected distance visual acuity (CDVA) was measured at a working distance of 5.5 m using the Pola VistaVision Visual Acuity Chart System (DMD Med Tech, Torino, Italy). The participants performed the visual tests using their best optical correction.

2.2. Filters

In order to analyze different levels of deterioration in the retinal-image quality, we used several filters. Five Bangerter foils (Ryser Optik, St Gallen, Switzerland) were used to worsen the retinal-image quality, graded 0.8, 0.6, 0.4, 0.3, and 0.2. Each value corresponds approximately to the theoretical visual acuity of the eye, in decimal notation, when seeing through the foil (taking into account an initial visual acuity of 1.0 or better). These foils present a pattern of microbubbles which produces the image degradation. Bangerter foils 0.8, 0.6, 0.4, 0.3 and 0.2 are characterized by a bubble density of 3.40, 3.41, 3.76, 3.44, and 4.32 bubbles/mm^2, respectively. They also present a bubble diameter of 0.26, 0.41, 0.22, 0.33, and 0.44 mm, respectively. Bangerter foils are of interest as they are employed in ocular penalization in children undergoing amblyopia therapy [25,26]. In addition, these filters are used to simulate visual degradation [24,27,28,31,32]. We also included different fog filters used in photography: the Black ProMist2 (Tiffen, Hauppauge, NY), the Fog A and the Fog B filters (HOYA, Kenko Tokina Co., Tokyo, Japan), a combination of the Fog A and Fog B filters (Fog_A + B), and the Fog_1 filter (B + W, Schneider, Bad Kreuznach, Germany). The structure of these filters is mainly characterized by their grain: the Fog_1 filter presents the smallest grain size, as well as the smallest grain density, and the Black ProMist 2 has the largest grain size but also greater variability in terms of the size and form of the grain.

Biomedical Optics EXPRESS

The Fog B filter produces a stronger fog effect than Fog A, which has a larger grain size. These camera filters, which produce an effect similar to dense fog, have been proved to provide visual acuity and contrast sensitivity values that can be used as cataract-simulating filters [23]. The Bangerter foils were fixed on ophthalmic lenses, with no optical power, previously mounted on eyewear frames: for each filter, a frame with the Bangerter foil affecting one eye was used. The fog filters were assembled on Knobloch K-2 shooting glasses (Knobloch Optik GmbH. Karlsruhe, Germany). To do this, a filter adapter was fitted onto the corresponding lens-holder of the shooting glasses. This frame allowed us to properly place the lens-holder with the fog filter in front of the eye. All the filters were analyzed beforehand, using an artificial eye used to calibrate the WASCA aberrometer (Carl Zeiss Meditec, AG, Germany), with a refractive error of +3.74D.

2.3. Retinal-image quality

Retinal-image quality was characterized using the OQAS II (Optical Quality Analysis System II, Visiometrics, Terrassa, Spain), a double-pass device widely validated in clinical practice [5,8] which uses an infrared laser diode (780 nm) as light source to obtain the double-pass images. The parameters measured were the Objective Scatter Index (OSI) and the Strehl ratio. The OSI parameter is obtained by analyzing the retinal image of a point source of light, calculated as the ratio between the light intensity within an annular area of 12 and 20 arc min and the intensity of the central peak (within 1 arc min) of the double-pass image [7]. This parameter is measured for a pupil diameter of 4 mm. The OSI objectively quantifies the intraocular scattering affecting the retinal image in such a way that a high OSI value indicates a greater contribution of intraocular scattering. OSI values lower than 1.0 correspond to normal eyes whereas cataractous eyes present OSI values of 1.0 and higher. The Strehl ratio provides information on the overall optical-quality and is defined as the ratio between the 2D Modulation Transfer Function (2D-MTF) area of the eye and the diffraction-limited 2D-MTF area. This parameter ranges from 0 to 1, where the higher the value, the fewer the ocular aberrations and scattering and, therefore, the better the retinal-image quality.

We first measured the optical quality of the artificial eye under normal conditions (without a filter). To do this, the artificial eye was fixed to the OQAS chinrest, following the manufacturer's instructions for the calibration process. We also measured the optical quality of the system comprising the artificial eye and a filter, for all the Bangerter foils and fog filters. We took three measurements and averaged these for each experimental condition. The data corresponded to a pupil diameter of 5 mm (Strehl ratio) and 4 mm (OSI). After this, both eyes of each participant were examined under natural conditions (with no filter), in addition to the system comprising the subject eye and a filter, for all the eyes and all the filters described (Bangerter foils and fog filters).

2.4. Visual discrimination capacity (halo perception)

The visual discrimination capacity under low ambient lighting was evaluated using the Halo test (http://hdl.handle.net/10481/5478, University of Granada, Granada, Spain), which is a visual test based on the freeware software Halo v1.0 [33] presented on a LCD-monitor. This test has been successfully used in clinical applications for ocular pathologies [6,11], after refractive surgery [20], and under different experimental conditions [34,35]. The test consists of detecting peripheral luminous stimuli (35 cd/m^2) around a central high-luminance stimulus (176 cd/m^2) under low-illumination conditions. This central stimulus is the source of the halo perception and other visual disturbances in low ambient lighting conditions, such as experienced in night vision. The size of the stimuli was configured using the radius: 30 pixels for the radius of the central stimulus and 1 pixel for the peripheral one, subtending 0.46 and 0.02 deg, respectively, from observer's position (2.5 m), which was fixed using a chinrest and the forehead. If none of the peripheral stimuli were detected, the radius was increased from 1 to 2 pixels, and so on. A total of 60 peripheral stimuli were randomly presented around the central one distributed along 12

Biomedical Optics EXPRESS

semi-meridians. The task of the patient was to detect (by clicking a mouse button) the peripheral stimuli presented on the monitor, maintaining fixation on the central stimuli. The information was stored and analyzed by the test software, providing a parameter, the visual disturbance index (VDI), which is calculated taking into account non-detected stimuli in relation to the total stimuli presented. This VDI ranged from 0 to 1 for the 1-pixel configuration, where the higher the VDI value, the lower the visual discrimination capacity in dim surroundings and, therefore, the stronger the halos perceived. This parameter is widely described in the literature [6,11,33–35]. If none of the peripheral stimuli were detected, VDI was 1; the peripheral-stimuli radius was increased from 1 to 2 pixels, and the test was performance again, as in other works [11], with the VDI ranging from 1 to 2 for this configuration, and so on.

2.5. Intraocular straylight

The intraocular straylight was measured using the C-Quant straylight meter (Oculus GmbH, Wetzlar, Germany). This device uses the psychophysical compensation comparison method and has been widely applied in clinical studies [23,36,37]. The metrics used was the straylight parameter, s, which describes the ratio between scattered light and the non-scattered light. The device reports the parameter log(s), which describes the ratio between scattered light and non-scattered light. The higher the log(s), the greater the forward intraocular straylight and, therefore, the stronger the luminous veil over the retinal image. The log(s) parameter increases with age, with values of about 0.90 found for young healthy eyes, 1.03 at 50 years of age, and 1.42 for 80-year-old patients, according to the normal straylight formula [9]. We took three measurements of straylight for each condition and averaged these. Only values meeting the reliability criterion were considered for the analysis (the expected standard deviation should be less than 0.08).

2.6. Contrast threshold

The contrast threshold (CT) was assessed using the contrast glare tester CGT-1000 (Takagi Seiko Co, Naganoken, Japan). This device measures 12-step contrast thresholds using a central luminous ring as a visual stimulus. To evaluate different spatial frequencies this luminous ring varies in size, subtending angles of 6.3, 4.0, 2.5, 1.6, 1.0, and 0.7 degrees from the observer position (0.35 m), corresponding to the spatial frequencies of 1.0, 1.7, 2.6, 4.2, 6.6, and 10.4 cycles per degree (cpd), respectively. The instrument is described in detail in the literature and it has various applications [38–40]. The CGT-1000 measures the contrast threshold with and without the presence of glare. The glare source used for this comprises 12 white LEDs distributed around the contrast stimulus at 11.8 deg. Three different glare levels are available: low, medium, and high. We used the high glare option (40000 cd/m^2) for the experiment. The CGT-1000 reports the contrast threshold with and without glare for the six spatial frequencies.

2.7. Procedures

The visual tests and ocular measurements of our subjects were performed monocularly in a random order, for both eyes, under natural viewing conditions and while wearing each of the Bangerter foils and fog filters. The filters were randomly assigned. Visual acuity (VA) was also included as a visual function in the study, which was evaluated along with visual discrimination capacity under low-illumination conditions, the contrast threshold, and straylight, as well as the ocular measurements (retinal-image quality). Visual acuity was determined in decimal notation using the Pola VistaVision Visual Acuity Chart System (DMD Med Tech, Torino, Italy) at distance (5.5 m). The experiment was split into different sessions to avoid subject fatigue (a session for each filter condition).

Biomedical Optics EXPRESS

2.8. Statistical analysis

For the data analysis, we used the SPSS 23.0 software (SPSS Inc., Chicago, IL). We verified the normal distribution of all the visual parameters measured (VA, OSI, Strehl ratio, VDI, log(s), and CT with and without glare) for our healthy young subjects, using the Shapiro-Wilk test (n=14). Then, an ANOVA test for repeated measures using Bonferroni correction was applied to analyze the effects of the different filters (Bangerter foils and fog filters) on the visual parameters measured. For the artificial eye (non-normal distribution), a Friedman test using a two-way ANOVA was run to analyze the OSI and Strehl ratio parameters for the different filters studied. Finally, for the human eyes, we performed several correlations analyses between VDI, OSI and log(s) using the Pearson correlation coefficient (r). Statistical significance was established for a p-value of 0.05 ($p<0.05$).

3. Results and discussion

The retinal-image quality data for the artificial eye is included in Table 1. The mean values for the objective scatter index (OSI) and the Strehl ratio under natural conditions (no filter) and with the different filters are shown. The OSI was significantly lower under natural conditions than with any of the Bangerter foils ($p<0.001$), although we found no differences when comparing this condition with any of the fog filters ($p=0.999$). The OSI for the artificial eye combined with any of the fog filters was significantly lower than with any of the Bangerter foils ($p<0.001$).

Table 1. Mean Strehl ratio and OSI values for the artificial eye and subject eyes

		Artificial eye		Subject eyes	
		OSI	Strehl ratio	OSI	Strehl ratio
No filter		0.0 ± 0.0	0.452 ± 0.003	0.5 ± 0.2	0.223 ± 0.057
Bangerter foils	BF_0.8	1.4 ± 0.3	0.073 ± 0.011	4.0 ± 0.4	0.074 ± 0.006
	BF_0.6	2.2 ± 0.6	0.081 ± 0.007	4.9 ± 1.3	0.082 ± 0.009
	BF_0.4	2.9 ± 0.3	0.065 ± 0.006	6.2 ± 1.4	0.064 ± 0.009
	BF_0.3	3.4 ± 0.3	0.064 ± 0.003	8.0 ± 1.2	0.058 ± 0.010
	BF_0.2	7.6 ± 1.0	0.055 ± 0.004	> 10.2	< 0.042
Fog filters	BMP2	0.1 ± 0.0	0.394 ± 0.020	0.8 ± 0.3	0.196 ± 0.051
	Fog_A	0.0 ± 0.0	0.440 ± 0.009	0.6 ± 0.3	0.194 ± 0.032
	Fog_B	0.0 ± 0.0	0.435 ± 0.006	0.6 ± 0.3	0.220 ± 0.048
	Fog_A + B	0.0 ± 0.0	0.432 ± 0.007	0.6 ± 0.3	0.212 ± 0.043
	Fog_1	0.0 ± 0.0	0.427 ± 0.007	0.6 ± 0.3	0.193 ± 0.036

For the Bangerter foils with the artificial eye, the OSI gradually worsened, on average, from natural conditions to BF_0.2 when following the expected order, with no significant differences being found between BF_0.6 and the other Bangerter foils ($p>0.05$), with exception of BF_0.2 ($p=0.027$). The greatest effect of the induced intraocular scattering was produced with the BF_0.2 foil, where OSI values comparable with a severe cataract were achieved, i.e., scattering levels similar to cataract group NO4 according to the lens opacities classification system (LOCS III) [7]. The Strehl ratio was significantly lower for the artificial eye with the Bangerter foils compared to natural conditions ($p<0.001$), but also compared to any of the fog filters ($p<0.001$), indicating a deterioration in the retinal-image quality. The highest level of retinal-image deterioration was found in the artificial eye with the BF_0.2 foil, followed by the artificial eye with the BF_0.3, with significant differences between the two conditions ($p<0.001$). For the fog filters, the most important degradation was achieved by the artificial eye with the BPM2 filter, with a significantly lower Strehl ratio than for natural conditions ($p<0.001$), but also lower than the artificial eye

Biomedical Optics EXPRESS

wearing the Fog_A (p=0.007) and Fog_B (p=0.036) filters. The Strehl ratio was also significantly lower for the artificial eye with the Fog_1 filter compared to the unfiltered condition (p=0.008), although no significant differences were found when comparing this with any of the other fog filter conditions (p>0.05).

Table 1 also includes the mean values for the retinal-image quality parameters (OSI and Strehl ratio) for the subjects' eyes under natural conditions and when wearing each of the Bangerter foils and the fog filters. Considering the OSI and the Strehl ratio, we found a significant deterioration in the retinal-image quality when comparing the subjects' eyes wearing any of the Bangerter foils with the natural conditions (p<0.001), excluding the human eyes combined with the BF_0.2 foil, where measurements could not be made due to the extreme deterioration of the retinal image. The OSI was significantly higher for all the fog filters compared to the unfiltered condition (p<0.05), except for Fog_1 (p=0.196).

We estimated a mean OSI value of greater than 10.2 for human eyes combined with the BF_0.2 foil, since the energy reaching the retina in this case was not high enough to report any results with OQAS for any of the eyes studied. This estimation is justified because the highest OSI value in our experiment was 10.2 for an eye wearing the BF_0.3 foil. For this reason, if measurements were possible, we would expect a significantly higher OSI with the eyes wearing the BF_0.2 foil compared to any of the other conditions studied. This estimation is supported by the results obtained for the artificial eye: the OSI was significantly higher with the BF_0.2 foil than the BF_0.3 foil (p< 0.001). According to the cataract classification ranges using the OSI parameter proposed by some authors [7], the mean OSI obtained for eyes combined with the BF_0.2 or BF_0.3 foil are comparable with severe cataracts. Furthermore, eyes wearing the BF_0.8, BF_0.6, and BF_0.4 foils are comparable with mature cataracts. For fog filters, only for eyes wearing the BPM2 did the OSI increase to values equating to early-stage cataracts. Some authors have reported that the BPM2 filter induces forward light scattering, providing a good approximation to early-stage cataracts [14,23]. The OSI values obtained in our experiment agree with this approximation and it is in line with the cataract classification proposed by Artal et al. [7], who reported an early cataract range of $1.0 \leq \text{OSI} \leq 3.0$, with a mean OSI for the control group of 0.7 ± 0.3. Our averaged baseline OSI was lower (0.5 ± 0.2) than this and we obtained a mean OSI of 0.8 ± 0.3 for eyes wearing the BPM2 filter, indicating increased intraocular scattering. It should be noted that significant dispersion in OSI values has been reported for patients classified according to the LOCS III classification, depending on the type of cataract [8].

For the Strehl ratio, a significant deterioration was recorded for subjects' eyes combined with any of the Bangerter foils compared to any of the fog-filters (p<0.001). For the BF_0.2 condition, we estimated a mean Strehl ratio of less than 0.042, which corresponds to the lowest value measured in the experiment. We would expect this parameter to be significantly lower than the unfiltered condition, as well as the fog filters, as demonstrated using the artificial eye.

Therefore, Bangerter foils and fog filters resulted in different levels of retinal-image degradation in real eyes (corroborated by an artificial eye) allowing us to analyze visual function under these conditions.

For visual function (Table 2), we found a significantly strong deterioration of all functions with respect to eyes under natural conditions (p<0.001). The visual discrimination capacity under low-illumination conditions significantly and progressively deteriorated for the eyes wearing the Bangerter foils (p<0.001), resulting in a stronger perception of halos and other night-vision disturbances. Statistically significant deteriorations (p<0.001) were found when comparing each foil against the others, except for the comparison of the BF_0.4 and BF_0.3 foils (p=0.476). This deterioration was also evident for the eyes when combined with the BPM2 (p<0.001), Fog_A + B (p=0.001) and Fog_A (p=0.002) filters. Eyes wearing the Fog_1 filter achieved a VDI similar to that recorded under natural conditions. These results are consistent with the night traffic scenes depicted in Fig. 1. The night scene viewed through the fog filters shows a predominance of

Biomedical Optics EXPRESS

circular halos (with no starburst disturbance), with the strongest halos present for the eyes wearing the Fog_A + B and BPM2 filters, in line with the VDI results (Table 2). The halos were weaker but larger for the Fog_1 filter compared to all the other fog filters, although there was a stronger luminous veil affecting the scene. Night vision disturbances were greater using the Bangerter foils. The night scene viewed through the Bangerter foils shows a specific light disturbance pattern depending on the structure of the foil (Fig. 2). As a result, the subject would perceive a combination of visual halos and starbursts affecting a larger area of the scene. A pattern of microbubbles can be appreciated with the Bangerter foils, shown in Fig. 2. The bubble density, as well as the shape and size of these bubbles, is related to the image degradation and night-vision disturbances perceived. The BF_0.2 and BF_0.3 foils generate a diffraction pattern compatible with that produced by a square aperture, which is comparable to the shape of the bubbles. The BF_0.8 foil shows the lowest density of bubbles, and their shape is approximately circular. Night vision disturbances induced by the BF_0.8, BF_0.6 and BF_0.4 foils are similar to those reported by some patients after refractive surgery, with a combination of halos and starbursts [41].

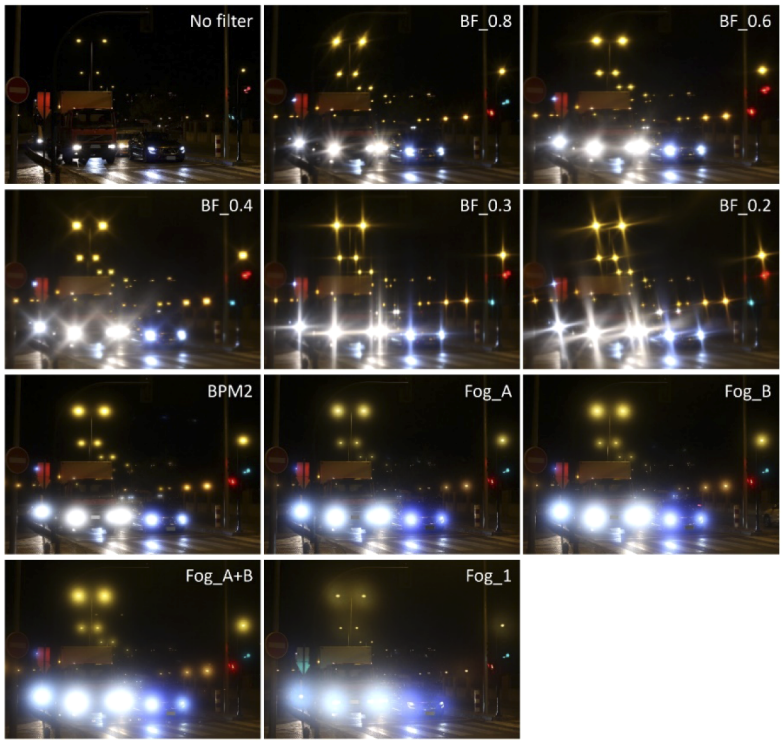

Fig. 1. Night traffic scene with no filter, and as perceived through each filter/foil studied. Each image corresponds to a photograph taken by a commercial camera (Canon EOS 650D) with no filter and using each of the filters/foils analyzed for a fixed configuration of the camera (f/5.6; 1/30 s; ISO 800, 40 mm).

On average, we found a good level of correspondence between the Bangerter foils and the expected visual acuities indicated by the manufacturer, with a standard deviation (SD) of 0.1, except for the BF_0.8 foil with a mean visual acuity of 0.7 ± 0.1 (Table 2). For the Bangerter foils, statistically significant differences were found compared to natural condition but also when comparing foils between them. With the exception of the BMP2 filter, no statistically significant differences were found when comparing the fog filters to each other ($p>0.05$).

Biomedical Optics EXPRESS

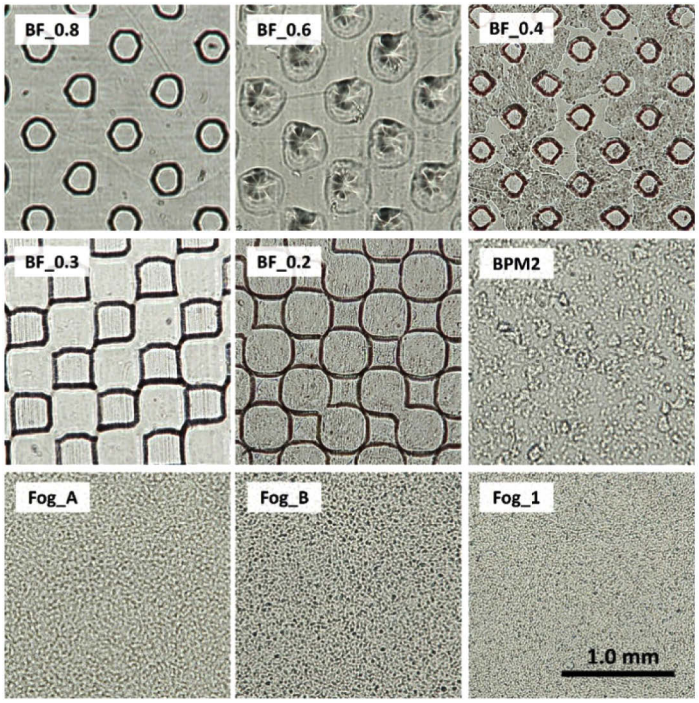

Fig. 2. Macro photographs of the patterns in the Bangerter foils and fog filters. using a commercial camera with a 40-mm lens and a 65-mm extension tube. The filters were illuminated using back-lighting (white LED). Each photograph corresponds to an area of 2×2 mm.

Table 2. Mean monocular values for the different visual functions studied in both eyes of the study subjects

		VA	VDI	log(s)
No filter		1.2 ± 0.1	0.19 ± 0.07	0.85 ± 0.05
Bangerter foils	BF_0.8	0.7 ± 0.1	0.59 ± 0.16	1.15 ± 0.14
	BF_0.6	0.6 ± 0.1	1.39 ± 0.25	1.38 ± 0.07
	BF_0.4	0.4 ± 0.1	1.55 ± 0.18	1.55 ± 0.06
	BF_0.3	0.3 ± 0.1	1.51 ± 0.15	1.53 ± 0.09
	BF_0.2	0.2 ± 0.1	2.59 ± 0.24	1.64 ± 0.05
Fog filters	BPM2	0.9 ± 0.1	0.33 ± 0.15	1.13 ± 0.08
	Fog_A	1.0 ± 0.2	0.32 ± 0.15	1.22 ± 0.15
	Fog_B	1.0 ± 0.2	0.24 ± 0.10	1.26 ± 0.08
	Fog_A + B	1.0 ± 0.1	0.35 ± 0.17	1.48 ± 0.07
	Fog_1	1.0 ± 0.1	0.20 ± 0.09	1.63 ± 0.07

The straylight was significantly lower for the eye in natural conditions compared to all the foils and filters ($p<0.001$), indicating a higher amount of forward scattering when any of the foils or filters studied were used. The highest mean log(s) was achieved by the eyes wearing the BF_0.2, followed by the eyes wearing the Fog_1 filter, with no statistical differences between these ($p=0.802$).

Biomedical Optics EXPRESS

The straylight increased, on average, in the following order: BPM2, BF_0.8, Fog_A, Fog_B, BF_0.6, Fog_A + B, BF_0.3, BF_0.4, Fog_1, and BF_0.2. Comparing each filter with the subsequent one in this list, statistical significant differences were revealed between Fog_B and BF_0.6 ($p<0.001$), BF_0.6 and Fog_A + B ($p=0.049$), and BF_0.4 and Fog_1 ($p=0.012$). The Fog_1 filter produced less halo effect than the rest of the filters (Table 2), enabling the most stimuli around the main luminous stimulus to be detected in the Halo test, although the amount of straylight was significantly greater than with the rest of the filters ($p<0.001$), excluding the BF_0.2 foil ($p=0.802$). These results agree with the night scenes shown in Fig. 1, since the shape and size of the streetlights is more precisely defined (softer but larger halos) in the scene corresponding to the Fog_1 filter. In addition, a veil of straylight can be observed affecting the Fog_1 scene, indicating that light from the streetlights is more scattered than with the other fog filters. The results for the Fog_A + B filter showed a strong halo perception (Fig. 1, Table 2) but also provided high straylight values, as can be appreciated in the night scenes (Fig. 1). The BPM2 filter provided the lowest straylight values of all the fog filters, although it did give a strong halo effect and higher OSI values. The corresponding night scenes agree with this assertion, since a softer veil of straylight can be seen than in those observed using the Fog_1 or Fog_A + B filters.

Considering the structure of the fog filters, characterized by their grain size (Fig. 2), it can be observed that the smaller the grain size of the filter, the greater the straylight effect and the lower the VDI. The smallest grain corresponds to the Fog_1 filter, for which the highest log(s) and lowest VDI values were reported of any of the fog filters. A similar tendency can be seen for the VDI of the Bangerter foils (see structure of the BF_0.8, BF_0.6, and BF_0.3 foils, whose microbubble density is almost the same).

Our visual acuity and straylight results for the fog filters are in line with those from other studies suggesting that the two parameters are rather independent of one another. This indicates that the visual acuity deterioration in cataracts is caused by aberrations and is not due to straylight [42]. We have corroborated this independence, since the visual acuity did not vary significantly between fog filters, with the exception of the BPM2 filter. For the Fog_1 filter, the log(s) values were close to those obtained for a grade 2 nuclear cataract (NO2) according to the LOCS III system [18].

Compared with natural conditions, the contrast threshold was, on average, significantly higher when wearing any of the filters studied ($p<0.001$), with the contrast sensitivity being strongly deteriorated for all spatial frequencies, especially with the Bangerter foils and the Fog_1 and BPM2 filters, as shown in Fig. 3. This deterioration was stronger in the presence of glare. In this condition, and while wearing the Bangerter foils (excluding BF_0.8), the participants did not detect the stimulus corresponding to the highest frequency (0.7 deg); they also did not detect this when wearing the Fog_1 filter. In addition, for the BF_0.2 foil with glare, the 1.0 deg stimulus was not detected (Fig. 1). The most important differences between the conditions studied in this work were achieved for the high spatial frequencies (low stimulus size); these differences were stronger under glare conditions. In the presence of glare, we found a significant deterioration of the contrast threshold in all the conditions studied compared to natural conditions ($p<0.001$). The results of previous studies have shown the relevance of contrast sensitivity and straylight for characterizing visual function, indicating that a deterioration in these variables can partially predict the performance of a visual task, such as driving [16], although when analyzing log(s) values in normal eyes, these authors obtained lower values (maximum mean value of 1.00) than reported in our work. Michael et al. also demonstrated the relevance of straylight when visually assessing drivers, observing that contrast sensitivity correlated well with the self-reported visual quality of drivers [43]. Other work has demonstrated that straylight (log(s)) is a good visual parameter for predicting simulated driving performance in both young and older people [16,44].

These results showed that retinal-image degradation negatively affects visual function. Understanding more about the correlation between this image degradation and visual function would

Biomedical Optics EXPRESS

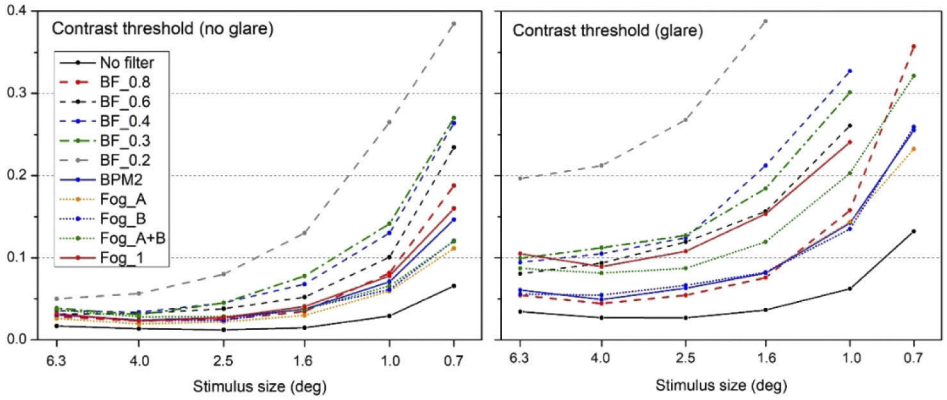

Fig. 3. The contrast threshold under normal illumination and under glare conditions as a function of stimulus size.

be of interest for clinical purposes, especially under low-illumination conditions, where the pupil dilates and the effect of the forward scattering on vision could be stronger. Figure 4 shows the results for the visual disturbance index (VDI) as a function of the scattering index (OSI) for all the conditions studied. Data for the BF_0.2 filter is plotted taking into account the fact that the OSI values in this condition are greater than 10.2 (see region with VDI > 2), as we have previously estimated. The OSI classification for cataracts proposed by Artal et al. has been highlighted in the graph [7]. This classification is in line with the results reported in other works [10,11]. We found a significant positive correlation ($r=0.903$, $p<0.001$) between the parameters analyzed (excluding the BF_0.2 condition). Therefore, the greater the intraocular scattering, the lower the visual discrimination capacity in dim lighting conditions, demonstrating a stronger influence of halos and other visual disturbances. The graphic results and data in Table 2 reveal a modest tendency towards a lower discrimination capacity with increased cataract severity, in terms of the OSI classification of cataracts. This is corroborated by the results for the BF_0.2 foil with the artificial eye, which presents the highest values of OSI and the highest VDI values for the observers' eyes. The data for the fog filters graphically locates in a similar area to that for natural conditions, although the highest OSI and VDI values for these filters were achieved with the BPM2 and Fog_A + B. Moreover, the VDI and OSI were, on average, higher for the fog filters than for natural conditions. For the Bangerter foils the VDI and OSI increased significantly, revealing a greater influence of induced scattering and perceived night-vision disturbances. Previous results have reported that a decrease in the Strehl ratio was associated with an increase in halo perception in patients after refractive surgery [20], as well as in older patients both with and without cataracts, whose OSI was also analyzed [11]. Recently, some authors have demonstrated that healthy eyes with a poorer retinal-image quality are related to larger halos [45]. They analyzed, among other things, the Strehl ratio and OSI, although the range of values analyzed was lower than in our results, and one of the limitations highlighted by the authors was that contrast sensitivity was not evaluated. Furthermore, in these studies, the maximum OSI measured was 2.3 [11], a value classified as being similar to an early-stage cataract ($1.0 \leq OSI \leq 3.0$) [7,46]. In our work, we obtained OSI values corresponding to all cataract classification groups, from normal eyes ($OSI < 1$) to severe cataracts ($OSI \geq 7.0$), analyzing a complete range of not only OSI values but also the Strehl ratio and all the visual functions studied.

On the other hand, Fig. 5 shows the influence of log(s) on the visual disturbance index for all the conditions studied. Two ranges of log(s) values are highlighted in the graph: normal eyes and cataractous eyes, according to the log(s) cutoff reported by Martínez-Roda [46]. We found a significant positive correlation ($r=0.866$, $p<0.001$) between the visual disturbance index (VDI)

Biomedical Optics EXPRESS

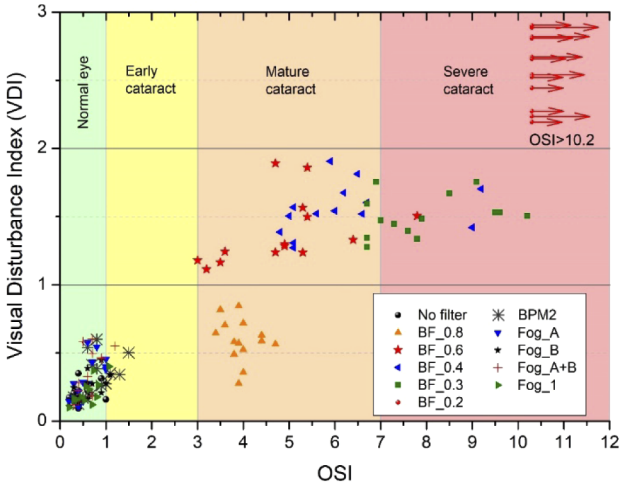

Fig. 4. The visual disturbance index (VDI) as a function of the scattering index (OSI) under the conditions studied.

and straylight for the Bangerter foils and natural conditions. However, we found no significant correlation for the fog filters (r=0.033, p=0.767), where only the BPM2 filter showed a significant increase in VDI. Puell et al. reported an ascending correlation between halo size and straylight in healthy eyes with a mean log(s) value of (0.95 ± 0.12), although the authors used a different visual test and metrics to evaluate halo perception [19]. In our work, we induced different degrees of visual deterioration and we observed a similar tendency for the Bangerter foils and natural conditions, but not for the fog filters. In addition, we analyzed a wider range of straylight values, with average log(s) values ranging from 0.85 to 1.64. Martinez-Roda et al. reported mean log(s) values of 1.49, 1.43, and 1.45 (SDs around 0.3) for nuclear, cortical, and posterior subcapsular cataract groups, respectively, and mean log(s) values of 1.22, 1.43, 1.55, and 1.83 (SDs around 0.2) for grades 1, 2, 3, and 4 of the LOCS III classification, respectively [46]. Michael et al. found a log(s) value of approximately 1.4 for mild cataracts [43]. Other authors analyzed straylight in early-stage nuclear and subcapsular cataracts, reporting mean log(s) values of 1.20 and 1.49 for nuclear (NO1 and NO2) and 1.13 and 1.25 for subcapsular (P1 and P2) cataracts, respectively [18]. In our work, we obtained mean log(s) values comparable to LOCS III grades of 1 (Fog_A, Fog_B), 2 (BF_0.6, Fog_A + B), 3 (Fog_A + B, BF_0.4, BF_0.3), and 4 (BF_0.2, Fog_1).

We also obtained a significant ascending correlation (r=0.870, p<0.001) between the log(s) values and the OSI for the Bangerter foils. Again, we found no significant ascending correlation for the fog filters (r=0.081, p=0.464), whereas the straylight did increase significantly for the different fog filter conditions. Some authors have reported a significant correlation between straylight and the OSI in healthy eyes, with log(s) values within a small range (from 0.70 to 1.03 for the straylight, and 0.90 to 1.59 for the OSI) [47]. Other authors have demonstrated that log(s) and OSI are good parameters for discriminating between cataractous eyes and healthy eyes for different cataract types according to the LOCS III classification [46]. However, these authors reported a disagreement between the two parameters, since the OSI is objectively measured with an artificial pupil of 4 mm and using a near-infrared light (780 nm), whereas log(s) is psychophysically measured using white light. Nevertheless, they did observe that the greatest differences between the two parameters were found in eyes with high scattering levels. Some studies have highlighted the limitation of the double-pass technique using an infrared light source, due to the large differences in double-pass images between infrared and green light [48,49], with the latter (550 nm) being where the human visual sensitivity almost reaches its maximum

Biomedical Optics EXPRESS

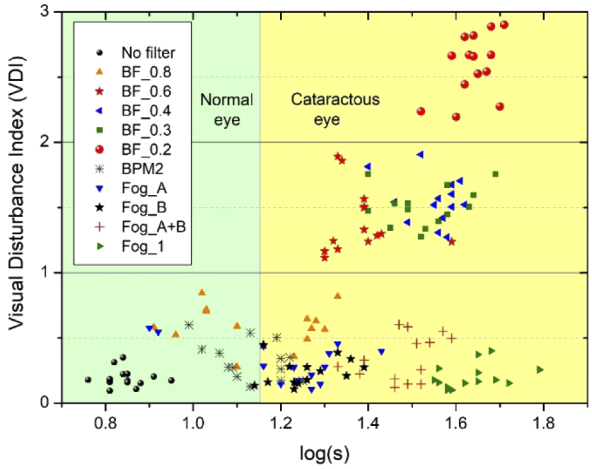

Fig. 5. The visual disturbance index (VDI) as a function of the straylight, log(s), under the conditions studied.

peak. These differences are principally due to the increased diffuse infrared light from the deeper layers of the retina, mainly from the choroid [48], contributing to the total scattered infrared-light in contrast to green light [50]. This agrees with the results for log(s) found by other authors analyzing different wavelengths, with the lowest and the highest values of log(s) being obtained for 550 and 800 nm, respectively [51], even though a different method for assessing the log(s) was utilized. These results are in line with other works that have demonstrated an important contribution of diffuse light from the fundus for wavelengths longer than 600 nm and small angles (0.5 deg), although such dependence appears weaker for larger angles [52]. However, in clinical practice, the use of infrared light contributes to patient comfort during the measurement, since green light typically causes after-images in patients [53]. Despite this limitation, the double-pass system used in this work has been shown to be a useful device for clinical purposes [2–7].

The OSI and log(s) represent objective and subjective intraocular forward scattering, respectively. The OSI parameter is calculated by analyzing the light intensity within an annular area of 12 and 20 arc min ("near-angle" scattering) with respect the central peak of the double-pass image [7]. Likewise, retinal straylight is measured for a visual angle of 5 to 10 deg using the compensation comparison method [47]. This angular difference, as well as the structure of the filters, could explain our findings for the fog filters, since the smallest-grain filter (Fog_1) provided the results with the highest log(s) value, i.e., the greatest amount of forward scattering (Table 2, Fig. 2) and, therefore, a higher luminous veil over the retinal image. However, for the fog filters, neither the Strehl ratio nor the OSI changed significantly compared to the natural condition, excluding the BPM2. These results reflect the limitation of the commercial double-pass device when measuring the scattering through small-grain (< 40 μm) filters with a uniform grain size, which produced a wider-angle scattering. This also was observed for the Strehl ratio, which was almost the same in the Fog_A, Fog_B, and combination of these (Fog_A + B), as the Strehl ratio includes contributions from intraocular scattering and aberrations working together. Ocular aberrations dominate the central peak of the Point Spread Function (PSF), while intraocular scattering occupies the peripheral part of the PSF (12-20 arcmin for the OSI calculation). These fog filters showed a low level of scattering influence with regard to the OSI parameter, as this double-pass device quantifies the 'near-angle' scattering and takes into account a background subtraction due to the contribution of diffuse infrared light from the fundus, making it less sensitive to the forward wide-angle scattering induced by these fog filters. In opposition, the log(s) resulted be more sensitive to forward scattering induced by fog filters, as well as the contrast

Biomedical Optics EXPRESS

threshold, especially under glare, as retinal straylight is strongly related to glare sensitivity. The BMP2 filter, which was the largest-grain fog filter (Fig. 2) and presented the most irregularity in terms of both grain size and form, provided, on average, the lowest log(s) values, although a significantly higher mean OSI value (and a lower Strehl ratio) was observed. This assertion agrees with the corresponding night scene for the Fog_1 filter (Fig. 1), where the shape of the streetlights can be appreciated in detail (not for the BMP2 filter). In this manner, lower OSI values were obtained for the Fog_1 than the BMP2 filter, since, taking into account a small angular distribution, the intensity within the annular area would be lower for the Fog_1 than the BMP2 filter. In the Halo test, the visual discrimination capacity was evaluated within 1 deg of visual angle, as in previous studies [33,54]. Taking into account our results, there are some conditions where the straylight and glare sensibility increases significantly but the OSI and the halo perception increases only slightly. Again, this is consistent with the night traffic scenes in Fig. 1, as well as our results for the fog filters (Table 2): the Fog_1 filter induced smoother and more diffuse halos with a stronger straylight effect on the scene, whereas the OSI did not change significantly compared to the unfiltered condition. Although the Fog_1 filter significantly affected the contrast sensitivity (especially under glare conditions), the study subjects were still able to detect peripheral stimuli in the Halo test. However, halo perception may be greater if the luminance of the peripheral stimuli was low enough, as demonstrated by other authors [19]. This luminance configuration restricts the VDI-log(s) correlation for the fog filters (Fig. 5), due, mainly, to wider-angle scattering compared to the other conditions (BF and BPM2); this creates a veil of straylight over the retinal image, which is better quantified by log(s). Under this condition, we would expect that the visual discrimination capacity would be poorer for the Fog_1 filter, since a higher number of peripheral stimuli would not be detected compared to the BMP2 filter condition.

Some authors have reported that camera filters like those used in this work provide visual acuity and contrast sensitivity values that simulate an early-stage cataract [23]. However, in that study, only BPM filters gave the desired cataract straylight values, something that was corroborated when the measurements were performed for only one subject with and without the BPM2 filter, using a research straylight-meter. In other work, Nicola et al. [55] studied scattered light through three different BPM filters (#1, #3 and #5) and for different wavelengths (405, 532, and 640 nm), finding stronger scattering for the shortest wavelength. They also evaluated vision (VA and CSF) in 10 eyes. Although they did not analyze the BPM2 filter, they found increasing deterioration of visual acuity and contrast sensitivity, especially for the highest frequency, from filters #1 to #5. These results are in line with our findings, with the deterioration of visual function for our BPM2 being close to that obtained for BPM3 by Nicola et al.

The Fog_1 filter gave higher log(s) values than the BPM2 filter for straylight angles of less than 10 deg. Other authors have also studied the scattering induced by BPM filters, finding a good correlation level between objective (OSI) and psychophysical evaluations of intraocular light scattering, with similar OSI values to those obtained in this work [56]. Our results for a total of 14 eyes, and using a commercial straylight-meter, have also demonstrated that BMP2 is the filter that best simulates an early-stage cataract, taking into account the straylight parameter and OSI values. In addition, we have also found that, using the Fog_A and Fog_B filters, the participants gave log(s) values comparable to an early-stage cataract, although the OSI values corresponded to normal values (non-cataractous eyes). For the Fog_1 filter, we obtained straylight levels comparable to a mature cataract (grades 2-3), although the OSI and VDI values were within the range of a normal eye, with both of them being slightly higher than in the unfiltered condition.

Puell et al. induced forward light scattering in young eyes using a BPM2 filter, demonstrating a deterioration in low-contrast vision and an increase in halo size [14]. However, a circular-disk halo was assumed due to the method used, which only measured halo sections of less than 60 deg. In our study, we analyzed the entire halo, i.e., 360 deg, allowing us to accurately quantify

Biomedical Optics EXPRESS

non-circular visual disturbances, such as those seen with some of the Bangerter foils in this work (Fig. 1), similar to the starbursts reported by some patients after refractive surgery [39]. Pérez et al. analyzed the optical properties of the 0.8, 0.6, 0.4, and 0.3 Bangerter foils [28]. They found that the structure and optical properties of the 0.6, 0.4, and 0.3 foils were similar, and not necessarily sequential, and only the 0.8 foil was substantially different. Our analysis found a better sequential correspondence between the foils, which were manufactured more recently, although the BF_0.4 and BF_0.3 foils did induce a similar visual function deterioration. It should be highlighted that the orthogonal patterns generated by the periodic structure of the Bangerter foils, especially for foils BF_0.3 and BF_ 0.2 (Fig. 1), differ from the starbursts reported by some cataract patients as a consequence of the diffraction caused by the irregularly shaped opacities within the crystalline lens. In this sense, the patterns generated by the BF_0.8 and BF_0.6 foils is closer to those reported by cataract sufferers and patients who have had corneal refractive surgery. Although Bangerter foils are not suitable for simulating cataracts, they do induce scattering levels comparable to different grades of cataracts.

In future work, it would be interesting to analyze other commercial filters, such as holographic diffusers, since the forward scatter profiles are usually provided by manufacturers, as well as to perform the Halo test using different levels of luminance for the peripheral stimuli.

4. Conclusion

Retinal image quality deterioration negatively affected visual performance for a range of degradation levels. Our results revealed that by inducing forward scattering, the higher the retinal-image degradation, the stronger the visual performance impairment. Increased forward scattering deteriorated the contrast threshold, especially under conditions of glare, as well as the visual discrimination capacity in night-vision conditions and glare sensibility, increasing the perception of halos and other visual disturbances. Bangerter foils induced forward scattering levels equivalent to mature to severe cataracts, and the night-vision disturbances were a combination of halos and starbursts, with these disturbances usually being reported by patients who have undergone ocular surgery or who suffer an ocular pathology. With respect to the OSI parameter, fog filters induced lower levels of forward scattering, and less severe night-vision disturbances, involving a combination of luminous veils and circular halos. The fog filters with the smallest grain size structure induced a very strong straylight effect, although the OSI values were analogous to those recorded under natural conditions. The BPM2 filter induced forward scattering comparable to an early-stage cataract, and the Fog_1 filter produced a very strong luminous veil effect characterized by high log(s) values due to more diffuse straylight distribution on the retinal image, showing the advantage of this measure for evaluating wide-angle scattering induced by small grained fog filters.

The visual discrimination capacity under all the viewing conditions and for a wide range of VDI and OSI values correlated well with the intraocular scattering according to the OSI parameter: the greater the intraocular scattering, the poorer the visual discrimination capacity and the stronger the halo perception and other night-vision disturbances. The Bangerter foils induced a stronger deterioration of the retinal image than the fog filters, mainly due to the structure of the filters.

In this sense, our findings could be of particular interest in the early stages of some ocular pathologies, like cataracts. In these cases, certain visual characteristics remain approximately stable, such as visual acuity, but forward scattering could strongly affect night vision, limiting the performance of some daily tasks, like night driving, or visual tasks in the presence of a glare source. The results of this work could therefore be of interest in clinical and research applications, to help understand how different levels of retinal-image deterioration influence visual performance and the early diagnosis of various ocular pathologies (like cataract), where ocular scattering affects the retinal image. In addition, our results provide a complete evaluation

Biomedical Optics EXPRESS

of the different visual disturbances, showing high levels of correlation between night-vision performance and retinal-image quality. This study could also be useful for more accurately determining the visual effects generated by the Bangerter foils when employed in amblyopia treatment for children.

Funding. Ministerio de Economía y Competitividad (FIS2017-85058-R).

Acknowledgments. We thank Trágora SCA for reviewing the English version of the manuscript.

Disclosures. The authors declare no conflicts of interest.

Data availability. Data underlying the results presented in this paper are not publicly available at this time but may be obtained from the authors upon reasonable request.

References

1. J. L. Alio, B. Elkady, D. Ortiz, and G. Bernabeu, "Clinical outcomes and intraocular optical quality of a diffractive multifocal intraocular lens with asymmetrical light distribution," J. Cataract Refractive Surg. **34**(6), 942–948 (2008).
2. J. C. Ondategui, M. Vilaseca, M. Arjona, A. Montasell, G. Cardona, J. L. Guell, and J. Pujol, "Optical quality after myopic photorefractive keratectomy and laser in situ keratomileusis: Comparison using a double-pass system," J. Cataract Refractive Surg. **38**(1), 16–27 (2012).
3. X. W. Xiao, J. Hao, H. Zhang, and F. Tian, "Optical quality of toric intraocular lens implantation in cataract surgery," Int. J. Ophthalmol. **8**(1), 66–71 (2015).
4. T. Liu, G. T. Lu, K. J. Chen, Q. X. Kan, and J. Bai, "Visual and optical quality outcomes of SMILE and FS-LASIK for myopia in the very early phase after surgery," BMC Ophthalmol. **19**(1), 88 (2019).
5. C. Ortiz, J. R. Jimenez, F. Perez-Ocon, J. J. Castro, and R. G. Anera, "Retinal-image quality and contrast-sensitivity function in age-related macular degeneration," Curr. Eye Res. **35**(8), 757–761 (2010).
6. J. J. Castro, J. R. Jimenez, C. Ortiz, A. Alarcon, and R. G. Anera, "New testing software for quantifying discrimination capacity in subjects with ocular pathologies," J. Biomed. Opt. **16**(1), 015001 (2011).
7. P. Artal, A. Benito, G. M. Perez, E. Alcon, A. De Casas, J. Pujol, and J. M. Marin, "An objective scatter index based on double-pass retinal images of a point source to classify cataracts," PLoS One **6**(2), e16823 (2011).
8. M. Vilaseca, M. J. Romero, M. Arjona, S. O. Luque, J. C. Ondategui, A. Salvador, J. L. Guell, P. Artal, and J. Pujol, "Grading nuclear, cortical and posterior subcapsular cataracts using an objective scatter index measured with a double-pass system," Br. J. Ophthalmol. **96**(9), 1204–1210 (2012).
9. T. Van den Berg, L. J. Van Rijn, R. Michael, C. Heine, T. Coeckelbergh, C. Nischler, H. Wilhelm, G. Grabner, M. Emesz, R. I. Barraquer, J. E. Coppens, and L. Franssen, "Straylight effects with aging and lens extraction," Am. J. Ophthalmol. **144**(3), 358–363.e1 (2007).
10. J. A. Martinez-Roda, M. Vilaseca, J. C. Ondategui, M. Aguirre, and J. Pujol, "Effects of aging on optical quality and visual function," Clin. Exp. Optom. **99**(6), 518–525 (2016).
11. C. Ortiz, J. J. Castro, A. Alarcon, M. Soler, and R. G. Anera, "Quantifying age-related differences in visual-discrimination capacity: drivers with and without visual impairment," Appl. Ergon. **44**(4), 523–531 (2013).
12. E. J. Patterson, G. Bargary, and J. L. Barbur, "Understanding disability glare: light scatter and retinal illuminance as predictors of sensitivity to contrast," J. Opt. Soc. Am. A **32**(4), 576–585 (2015).
13. N. I. Fan-Paul, J. Li, J. S. Miller, and G. J. Florakis, "Night vision disturbances after corneal refractive surgery," Surv. Ophthalmol. **47**(6), 533–546 (2002).
14. M. Cinta Puell and C. Palomo-Alvarez, "Effects of light scatter and blur on low-contrast vision and disk halo size," Optom. Vis. Sci. **94**(4), 505–510 (2017).
15. A. Lorente-Velazquez, A. Nieto-Bona, C. V. Collar, and A. G. Mesa, "Straylight and contrast sensitivity after corneal refractive therapy," Optom. Vis. Sci. **88**(10), 1245–1251 (2011).
16. M. Casares-Lopez, J. J. Castro-Torres, F. Martino, S. Ortiz-Peregrina, C. Ortiz, and R. G. Anera, "Contrast sensitivity and retinal straylight after alcohol consumption: effects on driving performance," Sci. Rep. **10**(1), 13599 (2020).
17. L. Franssen, J. Tabernero, J. E. Coppens, and T. J. T. P. van den Berg, "Pupil size and retinal straylight in the normal eye," Invest. Ophthalmol. Visual Sci. **48**(5), 2375–2382 (2007).
18. C. P. Filgueira, R. F. Sanchez, L. A. Issolio, and E. M. Colombo, "Straylight and visual quality on early nuclear and posterior subcapsular cataracts," Curr. Eye Res. **41**(9), 1209–1215 (2016).
19. M. C. Puell, M. J. Perez-Carrasco, C. Palomo-Alvarez, B. Antona, and A. Barrio, "Relationship between halo size and forward light scatter," Br. J. Ophthalmol. **98**(10), 1389–1392 (2014).
20. R. G. Anera, J. J. Castro, J. R. Jimenez, C. Villa, and A. Alarcon, "Optical quality and visual discrimination capacity after myopic LASIK with a standard and aspheric ablation profile," J. Cataract Refractive Surg. **27**(8), 597–601 (2011).
21. R. S. Anderson, T. Redmond, D. R. McDowell, K. M. M. Breslin, and M. B. Zlatkova, "The robustness of various forms of perimetry to different levels of induced intraocular stray light," Invest. Ophthalmol. Visual Sci. **50**(8), 4022–4028 (2009).
22. G. Ikaunieks, M. Colomb, and M. Ozolinsh, "Light scattering in artificial fog and simulated with light scattering filter," Ophthalmic Physiol. Opt. **29**(3), 351–356 (2009).

Biomedical Optics EXPRESS

23. G. C. de Wit, L. Franssen, J. E. Coppens, and T. van den Berg, "Simulating the straylight effects of cataracts," J. Cataract Refractive Surg. **32**(2), 294–300 (2006).
24. N. V. Odell, D. A. Leske, S. R. Hatt, W. E. Adams, and J. M. Holmes, "The effect of Bangerter filters on optotype acuity, Vernier acuity, and contrast sensitivity," J. AAPOS **12**(6), 555–559 (2008).
25. C. E. Stewart, M. J. Moseley, D. A. Stephens, A. R. Fielder, and M. Cooperative, "Treatment dose-response in amblyopia therapy: The Monitored Occlusion Treatment of Amblyopia Study (MOTAS)," Invest. Ophthalmol. Visual Sci. **45**(9), 3048–3054 (2004).
26. R. P. Rutstein, and G. Pediatric Eye Dis Investigator, "A randomized trial comparing Bangerter filters and patching for the treatment of moderate amblyopia in children," Ophthalmology **117**(5), 998–1004.e6 (2010).
27. N. V. Odell, S. R. Hatt, D. A. Leske, W. E. Adams, and J. M. Holmes, "The effect of induced monocular blur on measures of stereoacuity," J. AAPOS **13**(2), 136–141 (2009).
28. G. M. Perez, S. M. Archer, and P. Artal, "Optical characterization of Bangerter foils," Invest. Ophthalmol. Visual Sci. **51**(1), 609–613 (2010).
29. J. A. Martinez-Roda, C. E. Garcia-Guerra, F. Diaz-Douton, J. Pujol, A. Salvador, and M. Vilaseca, "Quantification of forward scattering based on the analysis of double-pass images in the frequency domain," Acta Ophthalmol. **97**(7), E1019–E1026 (2019).
30. A. D. Hwang, M. Tuccar-Burak, R. Goldstein, and E. Peli, "Impact of oncoming headlight glare with cataracts: a pilot study," Front. Psychol. **9**, 164 (2018).
31. A. Kingsnorth, T. Drew, B. Grewal, and J. S. Wolffsohn, "Mobile app Aston contrast sensitivity test," Clin. Exp. Optom. **99**(4), 350–355 (2016).
32. R. Molina, B. Redondo, L. L. DiStasi, R. G. Anera, J. Vera, and R. Jiménez, "The short-term effects of artificially-impaired binocular vision on driving performance," Ergonomics **64**(2), 212–224 (2021).
33. J. J. Castro, C. Ortiz, A. M. Pozo, R. G. Anera, and M. Soler, "A visual test based on a freeware software for quantifying and displaying night-vision disturbances: study in subjects after alcohol consumption," Theor. Biol. Med. Model. **11**(S1), S1 (2014).
34. J. J. Castro, A. M. Pozo, M. Rubino, R. G. Anera, and L. Jimenez del Barco, "Retinal-image quality and night-vision performance after alcohol consumption," J. Ophthalmol. **2014**, 1–7 (2014).
35. J. J. Castro, M. Soler, C. Ortiz, J. R. Jimenez, and R. G. Anera, "Binocular summation and visual function with induced anisocoria and monovision," Biomed. Opt. Express **7**(10), 4250–4262 (2016).
36. T. van den Berg, L. Franssen, and J. E. Coppens, "Straylight in the human eye: testing objectivity and optical character of the psychophysical measurement," Ophthalmic Physiol. Opt. **29**(3), 345–350 (2009).
37. G. Labuz, N. Lopez-Gil, T. van den Berg, and F. Vargas-Martin, "Ocular straylight with different multifocal contact lenses," Optom. Vis. Sci. **94**(4), 496–504 (2017).
38. K. Pesudovs, "Takagi Glare Tester CGT-1000 for contrast sensitivity and glare testing in normal individuals and cataract patients," J. Cataract Refractive Surg. **23**(5), 492–498 (2007).
39. P. P. Ye, X. Li, and K. Yao, "Visual outcome and optical quality after bilateral implantation of aspheric diffractive multifocal, aspheric monofocal and spherical monofocal intraocular lenses: a prospective comparison," Int. J. Ophthalmol. **6**(3), 300–306 (2013).
40. C. Ortiz, S. Ortiz-Peregrina, J. J. Castro, M. Casares-Lopez, and C. Salas, "Driver distraction by smartphone use (WhatsApp) in different age groups," Accid. Anal. Prev. **117**, 239–249 (2018).
41. S. D. Klyce, "Night vision disturbances after refractive surgery: haloes are not just for angels," Br. J. Ophthalmol. **91**(8), 992–993 (2007).
42. T. van den Berg, "The (lack of) relation between straylight and visual acuity. Two domains of the point-spread-function," Ophthalmic Physiol. Opt. **37**(3), 333–341 (2017).
43. R. Michael, L. J. van Rijn, T. van den Berg, R. I. Barraquer, G. Grabner, H. Wilhelm, T. Coeckelbergh, M. Emesz, P. Marvan, and C. Nischler, "Association of lens opacities, intraocular straylight, contrast sensitivity and visual acuity in European drivers," Acta Ophthalmol. **87**(6), 666–671 (2009).
44. S. Ortiz-Peregrina, C. Ortiz, M. Casares-Lopez, J. J. Castro-Torres, L. Jimenez del Barco, and R. G. Anera, "Impact of age-related vision changes on driving," Int. J. Environ. Res. Public Health **17**(20), 7416 (2020).
45. L. Yao, Y. Xu, T. Han, L. Qi, J. Shi, Z. Zou, and X. Zhou, "Relationships between haloes and objective visual quality in healthy eyes," Transl. Vis. Sci. Technol. **9**(10), 13 (2020).
46. J. A. Martinez-Roda, M. Vilaseca, J. C. Ondategui, L. Almudi, M. Asaad, L. Mateos-Pena, M. Arjona, and J. Pujol, "Double-pass technique and compensation-comparison method in eyes with cataract," J. Cataract Refractive Surg. **42**(10), 1461–1469 (2016).
47. A. Iijima, K. Shimizu, H. Kobashi, A. Saito, and K. Kamiya, "Repeatability, reproducibility, and comparability of subjective and objective measurements of intraocular forward scattering in healthy subjects," BioMed Res. Int. **2015**, 1–6 (2015).
48. T. J. T. P. van den Berg, "To the the editor: Intra- and intersession repeatability of a double-pass instrument," Optom. Vis. Sci. **87**(11), 920–921 (2010).
49. T. J. T. P. van den Berg, "Problem of double pass recording using infrared light," Clin. Exp. Optom. **94**(4), 393 (2011).
50. N. López-Gil and P. Artal, "Comparison of double-pass estimates of the retinal-image quality obtained with green and near-infrared light," J. Opt. Soc. Am. A **14**(5), 961–971 (1997).

Biomedical Optics EXPRESS

51. D. Christaras, H. Ginis, A. Pennos, and P. Artal, "Intraocular scattering compensation in retinal imaging," Biomed. Opt. Express **7**(10), 3996–4006 (2016).
52. H. S. Ginis, G. M. Pérez, J. M. Bueno, A. Pennos, and P. Artal, "Wavelength dependence of the ocular straylight," Invest. Ophthalmol. Visual Sci. **54**(5), 3702–3708 (2013).
53. M. Vilaseca and J. Pujol, "Problem of double pass recording using infrared light response," Clin. Exp. Optom. **94**(4), 393–395 (2011).
54. J. J. Castro, J. R. Jimenez, C. Ortiz, M. Casares-Lopez, and S. Ortiz-Peregrina, "The range of stereoscopic perception: influence of binocular summation, interocular differences in optical quality and halo perception," J. Mod. Opt. **64**(13), 1307–1314 (2017).
55. N. Rizzieri, M. Ozolinsh, and V. Karitans, "Merits of vision in presence of light scattering using Tiffen ProMist filters," Proc. SPIE **11553**, 115531P (2020).
56. P. A. Barrionuevo, E. M. Colombo, M. Vilaseca, J. Pujol, and L. A. Issolio, "Comparison between an objective and a psychophysical method for the evaluation of intraocular light scattering," J. Opt. Soc. Am. A **29**(7), 1293–1299 (2012).